

# Perturbative Formulation of Dispersion Contributions to Interaction Energy of van der Waals Systems of “Closed-Shell–Open-Shell” Type

VLADIMÍR LUKEŠ,<sup>1</sup> VILIAM LAURINC,<sup>1</sup> STANISLAV BISKUPIČ<sup>2</sup>

Departments of <sup>1</sup>Chemical Physics and <sup>2</sup>Physical Chemistry, Faculty of Chemical Technology, Slovak University of Technology, 812 37 Bratislava, Slovakia

Received 23 November 1997; accepted 11 January 1999

**ABSTRACT:** Restricted Hartree–Fock molecular orbitals have been used for the evaluation of dispersion contributions to the van der Waals interaction between closed-shell and open-shell systems represented by a simple Slater determinant. The dispersion energy has been computed for the ground state of He–H and He–O<sub>2</sub>. The dispersion energy contributions obtained in larger basis sets are comparable with multipole expansion data and with *ab initio* calculations reported in the literature. © 1999 John Wiley & Sons, Inc. J Comput Chem 20: 857–866, 1999

**Keywords:** dispersion energy; weak van der Waals complexes; He–H; He–O<sub>2</sub>

## Introduction

Long-range forces between atoms and molecules play an important role in a variety of physical phenomena, such as the equilibrium structure of molecular and rare-gas crystals, transport properties of gases and liquids, and low-en-

ergy scattering experiments. From a purely theoretical point of view, the long-range forces have the advantage of being a well-defined problem. Contributions to the interaction energy can be classified in two categories: (1) those of a classical origin and (2) those of a quantum-mechanical origin. Four of the most important terms are the electrostatic, induction, dispersion, and exchange-repulsion energies.<sup>1–5</sup> The origin of the first three contributions can be traced to monomer properties (permanent multipole moments and polarizabilities). The electrostatic induction energies are classical long-range contributions, first considered by

Correspondence to: V. Lukeš; e-mail: lukes@theochem.chtf.stuba.sk

Contract/grant sponsor: Slovak Grant Agency for Science; contract/grant numbers: VEGA 1/4205/97, VEGA 1/4199/97

Debye<sup>6</sup> and Keesom.<sup>7</sup> The exchange interaction energy is repulsive and it is a result of the Pauli principle, which forbids the electrons of one monomer to penetrate into the occupied space of the partner. It may be conceptually related to the electron charge densities of interacting monomers, which avoid each other. The dispersion energy was introduced by London<sup>8,9</sup> and has a long-range character. It originates from a mutual polarization of the electronic charge distributions of interacting monomers (interactions of instantaneous multipoles that are related to dynamic multipole polarizabilities). An additional type of interaction energy called the "charge transfer" energy is sometimes postulated.<sup>3,5</sup> So far, the term has eluded rigorous definition and is strongly dependent on the theoretical formalism and the basis set effects.

For the monomers without permanent dipole moments the dispersion forces dominate in the intermolecular attraction. They depend on their mutual orientations in nonsymmetric interacting systems. If the internuclear distance between two spherical symmetric atoms A and B is large, then the nonretarded potential energy,  $V_{AB}(R)$ , between them may be expressed as a power series of the inverse of distance  $R$ :

$$V_{AB}(R) = -C_6 R^{-6} - C_8 R^{-8} - C_{10} R^{-10} - \dots \quad (1)$$

where coefficient  $C_6$  describes the dipole-dipole interaction,  $C_8$  the dipole-quadrupole interaction, and  $C_{10}$  and the quadrupole-quadrupole and dipole-octupole interactions. Because the dipole-dipole interaction is dominant, it has attracted the greatest attention. Reliable numerical results for  $C_6$  are now available for a variety of van der Waals systems.<sup>3,10,11</sup> However, the accuracy of the  $C_8$  and  $C_{10}$  coefficients is much more difficult to determine because there are no direct experimental measurements of quadrupole and octupole polarizabilities.

The *ab initio* methods used for calculations of interaction energies can be classified as supermolecular, perturbational, and hybrid ones. In a supermolecular approach, the interaction energy is obtained as:

$$E_{\text{int}} = E_{AB} - E_A - E_B \quad (2)$$

where  $E_A$  ( $E_B$ ) and  $E_{AB}$  are approximations to the exact ground-state energies of the A (B) monomer and of the AB complex, respectively. It is clear that, in the supermolecular approach, the interaction energy is obtained as a single number. Its

decomposition into terms with clear physical meaning is not straightforward, and additional calculations are necessary for a better physical understanding of the interaction.<sup>5</sup>

The perturbational methods compute the interaction energy directly as the sum of distinct physical corrections:

$$E_{\text{int}} = E_{\text{elst}}^{(1)} + E_{\text{exch}}^{(1)} + E_{\text{ind}}^{(2)} + E_{\text{disp}}^{(2)} + E_{\text{exch}}^{(2)} + \dots \quad (3)$$

where  $E_{\text{elst}}^{(1)}$  is the classical electrostatic interaction energy,  $E_{\text{ind}}^{(2)}$  is the classical induction energy, and  $E_{\text{disp}}^{(2)}$  is the quantum-mechanical dispersion energy. The exchange-overlap corrections (subscript "exch") may be approximated by different ways.<sup>12-17</sup>

The intermolecular perturbation methods used to calculate the interaction energy contributions can be developed in the framework of the restricted (RHF) or unrestricted (UHF) Hartree-Fock approaches. The application of these approaches brings certain problems and advantages. The RHF solutions for open-shell monomers would provide the matrix element of the Hamiltonian which, in general, is not invariant with respect to orthogonalization procedures.<sup>18,19</sup> The use of the UHF wave function, in describing monomers and the dimer, brings forth the difficulties resulting from their different spin contamination.<sup>20</sup> Another common difficulty is that not only that the UHF procedure may fail to converge but it may converge to a symmetry-breaking solution.<sup>21</sup> The efficiency of the interaction energy components up to the second order of perturbation expansion using UHF treatment has been established recently for several open-shell cases.<sup>20-22</sup>

The aim of this work is to use single determinant restricted Møller-Plesset perturbation theory for the evaluation of the dominant dispersion contributions to the interaction energy of van der Waals systems of the "closed-shell-open-shell" type. The presented formulas are tested for the ground state of He-H and He-O<sub>2</sub> systems, which are bounded by the dispersion effect. The results are compared with the literature data.

## Theory

Let us consider two systems A and B forming together a composite quantum-mechanical system. The total Hamiltonian in the Møller-Plesset partitioning<sup>23</sup> for intermolecular problems<sup>24,25</sup> has the

form:

$$H_{AB} = F_A + F_B + W_A + W_B + V_{AB} \quad (4)$$

where  $F_X$  is the Fock operator and  $W_X$  the correlation (or fluctuation) potential for the system  $X = A, B$ . The mutual interaction between systems A and B is given by the perturbation term  $V_{AB}$ . The dispersion energy can be expressed via the expansion<sup>26–28</sup>:

$$E_{\text{disp}}^{(n)} = \sum E_{\text{disp}}^{(nij)} \quad (5)$$

where  $n$  is the order of perturbation  $V_{AB}$  and  $i$  ( $j$ ) indicates the order of the Møller–Plesset fluctuation potential for the A (B) system. A short description and the explicit formulas for the dispersion contributions in terms of molecular orbitals are presented in what follows. Single occupied orbitals are denoted by  $S$ , whereas  $D$  ( $V$ ) denote spaces over doubly occupied (virtual) orbitals. We consider that A corresponds to the closed-shell system and B to the open-shell system.

The separation of the  $E_{\text{disp}}^{(2)}$  terms can be performed easily by invoking the diagrammatic representation of perturbation theory corrections. In this section, we present the derivation and diagrammatic description of the  $E_{\text{disp}}^{(200)}$ ,  $E_{\text{disp}}^{(210)}$ ,  $E_{\text{disp}}^{(201)}$ , and  $E_{\text{disp}}^{(300)}$  contributions to the dispersion energy. We use the Goldstone-type diagrams (the second- and third-order type), and the orbital lines of the B(A) system are drawn conventionally above (below) the horizontal bar separating the monomers. The occupied (virtual) orbitals are labeled  $i, j, k, l$  ( $p, q, r, s$ ) indices, and  $\nu_{ij}^{pq}$  denotes the two-particle molecular integrals in the form  $\langle pq|ij \rangle$ . The symbol  $\omega_{ij}^{pq}$  corresponds to  $\nu_{ij}^{pq}/(\varepsilon_i + \varepsilon_j - \varepsilon_p - \varepsilon_q)$ , where  $\varepsilon_x$  are the orbital energies.

## SECOND-ORDER HARTREE–FOCK DISPERSION ENERGY

If the intramonomer correlation is completely neglected, then the dispersion energy may be approximated by  $E_{\text{disp}}^{(200)}$  (second-order HF dispersion energy). The corresponding diagram for this term is presented in Figure 1, and the final orbital expression is:

$$E_{\text{disp}}^{(200)} = \sum_{p,q} \sum_{i,j}^{un} \sum_{occ} D_1 \nu_{ij}^{pq} \omega_{ij}^{pq} \quad (6)$$

where the numerical factor  $D_1$  obtained from the spin summation is given in Table I. The above

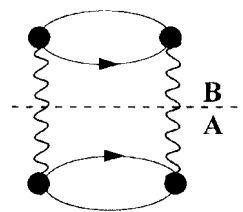


FIGURE 1. Diagrammatic representation for  $E_{\text{disp}}^{(200)}$ .

expression is very simple and the HF dispersion energy can also be calculated easily for larger polyatomic molecules.

## THIRD-ORDER HARTREE–FOCK DISPERSION ENERGY

The value of this correction indicates the rate of convergence for perturbation expansion in many-electron systems. This term is visualized by four Goldstone diagrams, which contain the pure Coulombic terms only (see Fig. 2a–d). The final orbital expression for the sum of particle–particle, particle–hole, hole–hole, and hole–particle interaction is:

$$\begin{aligned} E_{\text{disp}}^{(300)} = & \sum_{p,q,r,s}^{un} \sum_{i,j}^{occ} D_1 \omega_{ij}^{pr} \nu_{pr}^{qs} \omega_{ij}^{qs} \\ & - \sum_{p,q,r}^{un} \sum_{i,j,k}^{occ} D_2 \omega_{ij}^{pr} \nu_{ij}^{qj} \omega_{ik}^{qr} \\ & + \sum_{p,q}^{un} \sum_{i,j,k,l}^{occ} D_3 \omega_{ik}^{pq} \nu_{jl}^{ik} \omega_{jl}^{pq} \\ & - \sum_{p,q,r}^{un} \sum_{i,j,k}^{occ} D_4 \omega_{ik}^{pq} \nu_{jq}^{ir} \omega_{jk}^{pr} \end{aligned} \quad (7)$$

where the coefficients  $D_1$ – $D_4$  originating from the spin summations are given in Table II.

TABLE I. Multiplication Factors for  $E_{\text{disp}}^{(200)}$ .

$D_1$	System A		System B	
	$p$	$i$	$q$	$j$
4	V	D	V	D
2	V	D	V	S
2	V	D	S	D

FIRST-ORDER INTRAMONOMER CORRELATION CORRECTIONS

The leading intramonomer correlation correction to  $E_{\text{disp}}^{(2ij)}$  corresponds to the first-order perturbation in  $W_{\chi}$  and is represented by the sum of  $E_{\text{disp}}^{(210)}$  and  $E_{\text{disp}}^{(201)}$ . These terms describe the coupling of the intramonomer correlation effect with the intermolecular dispersion interaction. The diagrams that are assigned to the  $E_{\text{disp}}^{(210)}$  correction to the HF dispersion energy are shown in Figure 3a–f. We note that, by evaluating the diagrams (see Fig. 3a–f), using the symbols for border lines in parentheses, we obtain the algebraic representation for the term  $E_{\text{disp}}^{(201)}$ . The expansions of  $E_{\text{disp}}^{(210)}$  ( $E_{\text{disp}}^{(201)}$ ).

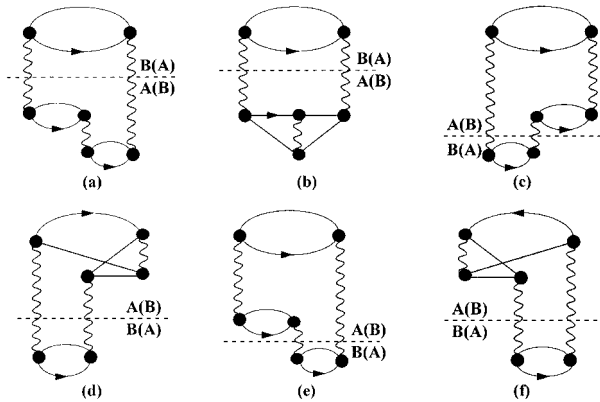


FIGURE 3. Diagrammatic representation for  $E_{\text{disp}}^{(210)}$  ( $E_{\text{disp}}^{(201)}$ ).

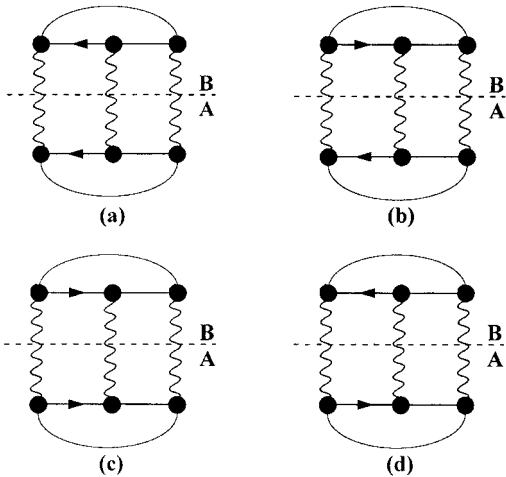


FIGURE 2. Diagrammatic representation for  $E_{\text{disp}}^{(300)}$ .

and  $E_{\text{disp}}^{(201)}$  in terms of molecular integrals can be performed using the standard diagrammatic technique and the final form of these terms is:

$$\sum_{p,q,r}^{un} \sum_{i,j,k}^{occ} \omega_{jk}^{qr} \omega_{ik}^{pr} (D_1 \nu_{ij}^{pq} - D_2 \nu_{qi}^{pj}) + \sum_{p,q,r}^{un} \sum_{i,j,k}^{occ} 2 \omega_{ik}^{pr} \omega_{jk}^{qr} (D_1 \omega_{ij}^{pq} - D_2 \omega_{ij}^{qp}) \quad (8)$$

The multiplication factors  $D_1$  and  $D_2$  for  $E_{\text{disp}}^{(210)}$  and  $E_{\text{disp}}^{(201)}$  are given in Table III. It should be stressed that the Figure 3c and d is algebraically identical to Figure 3e and f.

TABLE II. Multiplication Factors for  $E_{\text{disp}}^{(300)}$ .

System A							System B						
$D_1$	$p$	$q$	$i$	$r$	$s$	$j$	$D_2$	$p$	$q$	$i$	$r$	$j$	$k$
4	V	V	D	V	V	D	4	V	V	D	V	D	D
4	V	V	D	V	S	D	4	V	V	D	V	D	S
2	V	V	D	S	S	D	2	V	V	D	V	S	S
2	V	V	D	V	V	S	2	V	V	D	S	D	D
System A							System B						
$D_3$	$p$	$i$	$j$	$q$	$k$	$l$	$D_4$	$p$	$i$	$j$	$r$	$q$	$k$
4	V	D	D	V	D	D	4	V	D	D	V	V	D
4	V	D	D	V	D	S	4	V	D	D	V	S	D
2	V	D	D	S	D	D	2	V	D	D	V	V	S
2	V	D	D	V	S	S	2	V	D	D	S	S	D

**TABLE III.**  
**Multiplication Factors for  $E_{\text{disp}}^{(210)}$  and for  $E_{\text{disp}}^{(201)}$ .**

$E_{\text{disp}}^{(210)}$		System A				System B	
$D_1$	$D_2$	$p$	$q$	$i$	$j$	$r$	$k$
8	4	V	V	D	D	V	D
4	2	V	V	D	D	V	S
4	2	V	V	D	D	S	D

$E_{\text{disp}}^{(201)}$		System B				System A	
$D_1$	$D_2$	$p$	$q$	$i$	$j$	$r$	$k$
8	4	V	V	D	D	V	D
8	4	V	S	D	D	V	D
8	4	V	V	D	S	V	D
2	2	V	V	S	S	V	D
2	2	S	S	D	D	V	D
4	0	V	S	S	D	V	D

## Numerical Results

### He—H SYSTEM

The heteronuclear closed-shell–open-shell system He—H represents the simplest and an extremely weak van der Waals (vdW) complex. The knowledge of the interaction contributions and their properties for the He—H pair is also of interest in astrophysics. The absorption of infrared radiation by He—H is likely to be an important source of opacity of cooler stellar atmospheres.<sup>29,30</sup> A reliable empirical potential of He—H for the well region has been obtained by Jochemsen et al. ( $D_e = 22.03$  microhartrees [ $\mu\text{H}$ ] at  $R_e = 6.784$  bohr).<sup>31</sup> It is based on the low-temperature diffusion coefficients measured by Hardy et al.<sup>32</sup> A clarification from the theoretical point of view is very desirable, because the analysis of the experimental data has uncertainties. The diffusion cross-sections are measured with an accuracy of 5%, which leaves an uncertainty of about 10% for the potential.<sup>31</sup> The well energy of the Jochemsen empirical model<sup>31</sup> is about 20% deeper than the full CI *ab initio* calculation of Knowles et al. ( $D_e = 18.28$   $\mu\text{H}$  at  $R_e = 6.88$  bohr)<sup>33</sup> using a relatively large basis set. These authors felt confident enough to reject the empirical value of the well depth<sup>31</sup> on the basis of their computational results, along with a similarly deep well suggested by Scoles's so-called HFD-B (HF plus dispersion) model potential.<sup>34</sup> Two decades ago, Das et al.<sup>35</sup> performed

calculations at the MCSCF level. These calculations have not been corrected for the basis set superposition error (BSSE). It is known now that the MCSCF procedure employed slightly overestimates the bonding contributions in the well region.<sup>36</sup> The recently published *ab initio* calculations localized the vdW minimum at about 6.7 bohr, which is 22.6  $\mu\text{H}$  deep.<sup>30,36</sup> These results were obtained using large basis sets and the BSSE was eliminated.

The selection of the basis set for the description of vdW complexes is a very complicated task. The optimal basis set must contain polarization functions to describe the dispersion attractions and the BSSE must be made very small. In our work, four different basis sets are used. The B1–B3 sets represent augmented correlation consistent basis sets (aug-cc-PVDZ, aug-cc-PVTZ, aug-cc-PVQZ). The details of these sets have been given by Dunning and coworkers.<sup>37–39</sup> In addition, basis set B4, consisting of [6s5p4d3f] functions on helium and [6s3p2d1f] functions on hydrogen (g functions were omitted from the original basis sets of Meyer<sup>30</sup>) was used. This basis set was chosen for a better description of the dispersion interaction. All calculations were performed by the program codes developed in our laboratory and are interfaced with the G92 program system.<sup>40</sup> The Boys–Bernardi counterpoise correction was used<sup>41</sup> to eliminate BSSE from the supermolecular calculations. All calculations of the interaction contributions were done using dimer-centered basis sets.

The purpose of our study was not to obtain very accurate interaction energies, but rather to estimate the role of the developed dispersion energy contributions and the importance of term  $E_{\text{disp}}^{(200)}$  as an attractive part of the restricted second-order interaction correlation energy ( $\Delta E^{\text{RMP}2}$ ). However, it should be noted that the predicted position and depth of the minimum significantly depend on the basis set used. Their values converge monotonously with the increasing of basis set quality to the aforementioned literature data. At the MP2<sup>42,43</sup> level, we obtained  $D_e = 8.39$   $\mu\text{H}$  at  $R_e = 7.4$  bohr for B1, and  $D_e = 15.44$   $\mu\text{H}$  at  $R_e = 6.86$  bohr for B4.

The calculations have been performed for inter-system distances ( $R$ ) ranging from 5.5 to 10 bohr. In Table IV, the supermolecular interaction energy is separated into repulsive restricted HF interaction ( $\Delta E^{\text{RHF}}$ ) and attractive second-order correlation interaction ( $\Delta E^{\text{RMP}2}$ ) energies. In particular, the  $\Delta E^{\text{RHF}}$  is saturated with the present basis sets and the results are almost identical to the results of Meyer et al.<sup>30</sup> The so-called HF electrostatic

energy<sup>44–46</sup> can be evaluated easily for closed-shell and open-shell systems. The value of the HF electrostatic energy ( $E_{\text{els}}^{(100)}$ ) is almost insensitive to the basis set and, even for medium basis sets (B2), tends to the limit value (e.g.,  $E_{\text{els}}^{(100)} = -4.43 \mu\text{H}$  at  $R = 6.75$  bohr) and the ratio  $E_{\text{elst}}^{(100)}/\Delta E^{\text{RHF}}$  is about  $-0.229$  at the same distance. For comparison with a typical weak closed-shell van der Waals system, the limit HF interaction energy ( $\Delta E^{\text{HF}}$ ) for the  $\text{He}_2$  dimer at 5.6 bohr is  $29.196 \mu\text{H}$ ,<sup>47</sup> and  $E_{\text{elst}}^{(100)}/\Delta E^{\text{HF}}$  is approximately  $-0.169$ .<sup>48</sup>

The applicability of the evaluated contributions to the dispersion energy [see eqs. (6)–(8)] can be estimated from the data in Table IV.  $E_{\text{disp}}^{(200)}$  represents the leading term of the dispersion energy and the main attractive part of  $\Delta E^{\text{RMP2}}$ . The limit ratio,  $\Delta E^{\text{RMP2}}/E_{\text{disp}}^{(200)}$ , is about 0.94 at  $R = 6.75$  bohr. For  $\text{He—He}$  at  $R = 5.6$  bohr, the limit value for  $E_{\text{disp}}^{(200)}$  is found to be  $-54.095 \mu\text{H}$ ,<sup>49</sup> and the ratio  $\Delta E^{\text{RMP2}}/E_{\text{disp}}^{(200)}$  is approximately 0.93.<sup>47,48,50</sup> In our study, the total dispersion energy ( $E_{\text{disp}}$ ) is approximated as the sum  $E_{\text{disp}}^{(200)} + E_{\text{disp}}^{(210)} + E_{\text{disp}}^{(201)} + E_{\text{disp}}^{(300)}$ . The obtained results are compared with the data obtained from the multipole expansion [see eq. (1)]. The first three long-range coefficients  $C_6$ ,  $C_8$ , and  $C_{10}$  (2.823, 41.83, and 871.3 in atomic units, respectively) were taken from work of Koide et al.<sup>51</sup> The coefficient  $C_{12}$  (25512.3 a.u.) was obtained from the empirical recursion formula.<sup>30,52</sup>

As seen in Table IV, our dispersion energies (calculated with the B3 and B4 basis sets) are in agreement with the data from the multipole expansion and from MR–CI supermolecular calculations.<sup>30</sup> These results are slightly lower (about 7–9%) than the data obtained from MCSCF calculations.<sup>35</sup> The values in parentheses (Table IV) represent  $E_{\text{disp}}^{(300)}$ . The ratio ( $E_{\text{disp}}^{(300)}/E_{\text{disp}}^{(200)}$ ) is small and indicates a relatively good convergence of the perturbation expansion of the dispersion energy.

## He—O<sub>2</sub> SYSTEM

The triatomic vdW complexes containing the noble gas atom have been studied intensively in modern spectroscopic and scattering experiments. The stable ground state  $\text{He—O}_2$  complex has emerged as a convenient model for developing an *ab initio* strategy for interaction between closed-shell and open-shell species.<sup>53–55</sup>

The best empirical estimates of the global minimum parameters  $R_e$  and  $D_e$  for the T-shaped geometry are 6.18 bohr and  $119.8 \mu\text{H}$ <sup>53</sup> and 6.29 bohr and  $107.0 \mu\text{H}$ ,<sup>54</sup> respectively. No empirical

potentials reveals any local minimum for the linear orientation and the interaction energy varies monotonously between the linear and the T structure. However, the *ab initio* studies indicate the existence of secondary minima in the linear orientation. For example, Keil et al.<sup>56</sup> predict  $86.36 \mu\text{H}$  at 7.12 a.u., Faubel et al.<sup>54</sup>  $64.6 \mu\text{H}$  at 7.3 a.u., and Cybulski et al.<sup>21</sup>  $116.4 \mu\text{H}$  at 7.0 bohr, respectively. This discrepancy between experiment and theory might be explained by the fact that the experimental characterization of the secondary minima is much more difficult, because the scattering experiments efficiently probe only the primary minimum region.<sup>21</sup>

To compare the performance of the restricted versus unrestricted Møller–Plesset perturbation theory (MPPT) for the selected interaction energy contributions, we use the same geometries and 5s3p2d1f basis set for the O atom and 4s1p1d for the He atom as in the recent work of Cybulski et al.<sup>21</sup> The definition of the geometrical parameters of the  $\text{He—O}_2$  complex is the same as in their work<sup>21</sup>:  $R$  denotes the distance between the center of mass of the oxygen molecule and He atom, and  $\Theta$  corresponds to the angle between  $R$  vector and the  $\text{O}_2$  bond axis. The details of the basis sets used (denoted LD) are given in the Appendix of ref. 18.

According to Cybulski et al.,<sup>21</sup> the LD basis set at the UMP2 calculation level provides two minima:  $D_e = 81.3 \mu\text{H}$  at  $R_e = 6.0$  bohr for the T-shaped geometry and  $D_e = 79.5 \mu\text{H}$  at  $R_e = 7.4$  bohr for the linear geometry. The interaction energy calculated using the RPT2 level at  $R = 6.0$  bohr differs from the UHF spin-contaminated calculations. The minimum is slightly shifted ( $D_e = 71.1 \mu\text{H}$  at  $R_e = 6.4$  bohr). The projected UHF results are between the RHF and UHF data (see T structure in Table V).

Similar to the  $\text{He—H}$  vdW system, the interaction energy (in our case calculated at the MP2 level) is determined by the delicate balance between the repulsive HF and the attractive second-order correlation interaction energies. The selected interaction energy components obtained at the restricted and unrestricted MP2 level of the theory for angles varying from  $0^\circ$  to  $180^\circ$  (at  $R = 6$  bohr) are shown in Figure 4. The second-order interaction correlation energies ( $\Delta E^{\text{RMP2}}$  or  $\Delta E^{\text{UMP2}}$ ) reveal minima at  $\Theta = 0^\circ$  and  $180^\circ$ . The UHF calculations offer a very flat maximum in the middle of the oxygen bond. Similar to the closed-shell case, the difference between the second-order supermolecular interaction correlation and the HF dis-

TABLE IV.  
 $\Delta E^{\text{RHF}}$ ,  $\Delta E^{\text{RMP2}}$ , and Dispersion Contributions for He—H system (Energies in  $\mu\text{H}$ ).

$R$ (bohr)	Basis Set 1			Basis Set 2			Basis Set 3			Basis Set 4			MCSCF <sup>a</sup>		$E^{\text{RHF}} / \text{MR-Cl}^6$	ME <sup>c</sup>
	$\Delta E^{\text{RHF}}$	$-\frac{E_{\text{disp}}^{(200)}}{-\Delta E_{\text{RMP2}}^{(200)}}$	$-\frac{E_{\text{disp}}^{(300)}}{E_{\text{disp}}^{(300)}}$	$\Delta E^{\text{RHF}}$	$-\frac{E_{\text{disp}}^{(200)}}{-\Delta E_{\text{RMP2}}^{(200)}}$	$-\frac{E_{\text{disp}}^{(300)}}{E_{\text{disp}}^{(300)}}$	$\Delta E^{\text{RHF}}$	$-\frac{E_{\text{disp}}^{(200)}}{-\Delta E_{\text{RMP2}}^{(200)}}$	$-\frac{E_{\text{disp}}^{(300)}}{E_{\text{disp}}^{(300)}}$	$\Delta E^{\text{RHF}}$	$-\frac{E_{\text{disp}}^{(200)}}{-\Delta E_{\text{RMP2}}^{(200)}}$	$-\frac{E_{\text{disp}}^{(300)}}{E_{\text{disp}}^{(300)}}$	$\Delta E^{\text{RHF}}$	$-\frac{E_{\text{disp}}^{(200)}}{-\Delta E_{\text{RMP2}}^{(200)}}$	$-\frac{E_{\text{disp}}^{(300)}}{E_{\text{disp}}^{(300)}}$	$-\frac{C_{(6,8,10)}}{-C_{(6,8,10,12)}}$
5.50	199.39	96.32 (76.82)	126.87 (-0.07)	198.43	127.38 (105.73)	163.24 (2.40)	198.44	139.41 (116.36)	176.60 (4.16)	198.12	143.86 (120.34)	182.17 (4.95)	198.09	162.94	186.34 (219.64)	
6.00	79.60	56.24 (48.07)	74.48 (0.00)	78.74	71.88 (62.92)	93.10 (1.09)	78.82	78.01 (68.33)	99.97 (1.98)	78.73	81.79 (72.02)	105.08 (2.08)	78.4	81	94.64 (111.54)	
6.50	31.49	33.88 (30.45)	45.07 (0.02)	30.91	42.08 (38.39)	55.02 (0.49)	30.95	45.22 (41.48)	58.63 (0.88)	30.94	47.88 (43.86)	61.82 (1.19)	30.7	51	56.38 (61.52)	
6.75	19.74	26.61 (24.47)	35.47 (0.01)	19.31	32.66 (30.31)	42.87 (0.33)	19.32	34.92 (32.47)	45.54 (0.56)	19.33	37.07 (34.53)	48.17 (0.82)	19.32	43.96	43.99 (46.84)	
7.00	12.34	21.08 (19.62)	28.14 (0.01)	12.04	25.56 (24.07)	33.69 (0.22)	12.04	27.23 (25.76)	35.66 (0.39)	12.06	28.93 (27.27)	37.76 (0.57)	11.8	32	34.34 (36.18)	
7.50	4.79	13.55 (13.11)	18.13 (0.01)	4.66	16.14 (15.55)	21.39 (0.10)	4.65	17.04 (16.46)	22.49 (0.17)	4.66	18.07 (17.43)	23.77 (0.27)	4.6	21	21.59 (22.39)	
8.00	1.83	9.00 (8.74)	12.07 (0.00)	1.79	10.54 (10.32)	14.05 (0.02)	1.79	11.05 (10.76)	14.67 (0.08)	1.79	11.67 (11.40)	15.46 (0.12)	1.8	15	14.07 (14.44)	
10.0	0.04	2.28 (2.27)	3.06 (0.00)	0.04	2.53 (2.47)	3.39 (0.00)	0.04	2.60 (2.59)	3.49 (0.00)	0.04	2.69 (2.65)	3.58 (0.04)			3.31 (3.35)	

<sup>a</sup>MCSCF separation. <sup>35</sup> <sup>b</sup> $\Delta E^{\text{RHF}}$  and MR-Cl intra-atom correlation contributions (dispersion terms). <sup>30</sup> <sup>c</sup>Multipole expansion. Parameters  $C_6$ ,  $C_8$ , and  $C_{10}$  are taken from ref. 51,  $C_{12}$  obtained from the empirical recursion formula. <sup>30,52</sup>

**TABLE V.**  
**Energy Characteristics ( $\mu\text{H}$ ) of Two Minima<sup>21</sup>**  
**of He—O<sub>2</sub> Complex.<sup>a</sup>**

$R$ (bohr)	6.0	7.0
$\Theta$ ( $^\circ$ )	90	0 (180)
$\Delta E^{\text{RHF}}$	104.76	70.05
$\Delta E^{\text{RMP2}}$	−157.46	−157.89
$E_{\text{int}}^{(2)}$	−52.70	−87.84
$E_{\text{els}}^{(100)}$	−24.82	−16.79
$E_{\text{disp}}^{(200)}$	−212.86	−178.91
$E_{\text{disp}}^{(210)} + E_{\text{disp}}^{(201)}$	−17.61	−2.05
$E_{\text{disp}}^{(300)}$	1.82	1.45
$E_{\text{disp}}^{\text{UHF}}$	−228.65	−179.51
$\Delta E^{\text{UHF}}$	130.42 (141.56)	73.14 (74.81)
$\Delta E^{\text{UMP2}}$	−211.69 (−207.85)	−152.62 (−152.73)
$E_{\text{int}}^{(2)}$ (UHF)	−81.27 (−66.29)	−79.48 (−77.92)
$E_{\text{els}}^{(100)}$ (UHF)	−32.03	−17.40
$E_{\text{disp}}^{(200)}$ (UHF)	−210.89	−170.00

<sup>a</sup>UHF data obtained from the work Cybulski et al.,<sup>21</sup> and the values in parentheses represent the projected UHF results.

persion [ $E_{\text{disp}}^{(200)}$  or  $E_{\text{disp}}^{(200)}$  (UHF)] energies contains mainly the second-order electrostatic correlation energy, the second-order HF exchange-dispersion, and the deformation correlation contributions. These remaining terms are small near the T configuration and are negligible especially in the UHF approximation. The dispersion effect in the perpendicular orientation is small but it increases by increasing the deviation from 90°. However, the differences between  $E_{\text{disp}}^{(200)}$  and  $E_{\text{disp}}$  (see Fig. 4) reveal that contributions of the higher orders of

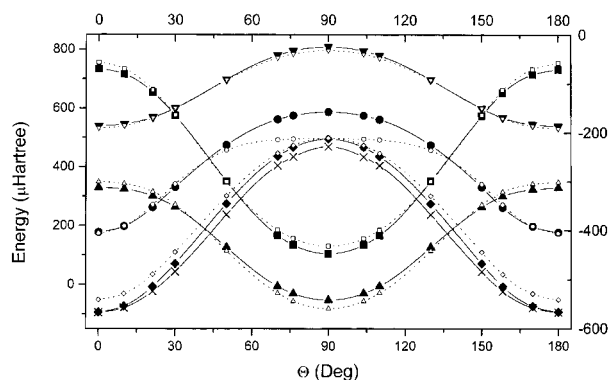


**FIGURE 4.** The  $\Theta$  dependence of RMP2 /UMP2 interaction energy and its selected components for the ground state He—O<sub>2</sub> system at  $R = 6.0$  bohr. UHF data taken from the work Cybulski et al.<sup>20</sup> The symbols for left y-axis: (■)  $\Delta E^{\text{RHF}}$ ; (□)  $\Delta E^{\text{UHF}}$ ; (▲)  $E_{\text{int}}^{(2)}$ ; (△)  $E_{\text{int}}^{(2)}$  (UHF). The symbols for right y-axis: (▼)  $E_{\text{els}}^{(100)}$ ; (▽)  $E_{\text{els}}^{(100)}$  (UHF); (◆)  $E_{\text{disp}}^{(200)}$ ; (◇)  $E_{\text{disp}}^{(200)}$  (UHF); (●)  $\Delta E^{\text{RMP2}}$ ; (○)  $\Delta E^{\text{UMP2}}$ ; (×)  $E_{\text{disp}} = E_{\text{disp}}^{(200)} + E_{\text{disp}}^{(210)} + E_{\text{disp}}^{(201)} + E_{\text{disp}}^{(300)}$ .

RHF dispersion energies decrease with increasing  $E_{\text{disp}}^{(200)}$ . The magnitude of the sum  $E_{\text{disp}}^{(201)} + E_{\text{disp}}^{(210)} + E_{\text{disp}}^{(300)}$  is  $-0.76 \mu\text{H}$  at  $\Theta = 0^\circ$  ( $180^\circ$ ) and  $-15.79 \mu\text{H}$  at  $\Theta = 90^\circ$ . The data in Table V indicate the same trend.

The HF electrostatic terms [ $E_{\text{els}}^{(100)}$  and  $E_{\text{els}}^{(100)}$  (UHF)] show an angular dependence with a maximum at 90° and minima at 0° and 180°. They are of a pure charge-overlap nature in the present case and show distinct flattening in the linear configuration. The shape of both curves is in agreement with the contour maps analysis of Bader and Esen.<sup>57</sup>

## Summary and Conclusions

In this study, we have presented explicit formulas for select contributions to the dispersion energy in terms of orbitals generated by the RHF-SCF procedure for nondegenerate closed-shell and open-shell van der Waals systems. The basis set dependence of the presented dispersion energy terms was tested for the He—H system. The numerical results indicate that the “best” values of  $E_{\text{disp}}^{(200)}$  near the vdW minimum represent roughly 79% of the value obtained from the multipole expansion. The  $E_{\text{disp}}^{(210)}$  and  $E_{\text{disp}}^{(201)}$  terms were much more difficult to calculate than  $E_{\text{disp}}^{(200)}$ , because they require additional calculations of the molecular integrals for separated A and B systems [see eq. (8)]. However, the importance of these terms and of the exchange-dispersion contributions is quite significant (about 25%). To obtain more precise results for the total dispersion energy, the selection of a better basis set, as well as inclusion of higher terms to the dispersion energy and exchange-dispersion energy is necessary. These terms can be evaluated by the presented diagrammatic scheme or by a suitable version of the coupled cluster method.<sup>58,59</sup>

The angular anisotropy and the performance of the restricted versus unrestricted MP2 interaction energy contributions was discussed for the triatomic vdW complex He—O<sub>2</sub> at  $R = 6.0$  bohr. The obtained RHF and UHF results were of comparable quality for the HF interaction, HF electrostatic, and second-order HF dispersion energies. However, significant differences were observed for second-order interaction correlation energies in the T-shaped structure.  $\Delta E^{\text{RMP2}}$  and  $\Delta E^{\text{UMP2}}$  may differ mainly in the exchange- and electrostatic-correlation energies. It is necessary to emphasize that



the UHF values were spin contaminated and thus the physical reliability of the interaction energy contributions may be questionable and spin projection or annihilation techniques may be desirable.

Finally, we conclude that a qualitatively correct description of the dispersion energy (near the vdW minimum) for interacting systems of the closed-shell–open-shell type, together with relatively small computational costs, suggest that the MBPT formalism presented offers a possible alternative to unrestricted MPPT treatment.

## Acknowledgments

The authors thank Professor V. Kvasnička for stimulating discussions and the referees for critical and inspiring remarks.

## References

- Claverie, P. From diatomic to biopolymers. In: Pullman, B., ed., *Intermolecular Interactions*; Wiley: New York, 1978.
- Jeziorski, B.; Kolos, W. In: Ratajczak, H.; Orville-Thomas, W. J., eds., *Molecular Interactions*, Vol. 3; Wiley: New York, 1982.
- Hobza, P.; Zahradník, R. *Chem Rev* 1988, 88, 871.
- Chalasinski, G.; Gutowski, M. *Chem Rev* 1988, 88, 943.
- Chalasinski, G.; Szczesniak, M. M. *Chem Rev.* 1994, 94, 1723.
- Debye, P. *Phys Z* 1920, 21, 178.
- Keesom, W. H. *Phys Z* 1921, 22, 129.
- London, F. *Z Phys Chem B* 1930, 11, 222.
- London, F. *Trans Faraday Soc* 1937, 33, 8.
- Tang, K. T.; Norbeck, J. M.; Certain, P. R. *J Chem Phys* 1976, 64, 3063.
- Buckingham, A. D.; Fowler, P. W.; Hutson, J. M. *Chem Rev* 1988, 88, 963.
- Rybak, S.; Jeziorski, B.; Szalewicz, K. *J Chem Phys* 1991, 95, 6576.
- Moszynski, R.; Jeziorski, B.; Szalewicz, K. *J Chem Phys* 1994, 100, 1312.
- Basilevsky, M. V.; Berenfeld, M. M. *Int J Quantum Chem* 1972, 6, 23.
- Daudey, J. P.; Claverie, P.; Malrieu, J. P. *Int J Quantum Chem* 1974, 8, 1.
- Mayer, I. *Int J Quantum Chem* 1983, 23, 341.
- Laurinc, V.; Lukeš, V.; Biskupič, S.; *Theor Chem Acc* 1998, 99, 53.
- van Lenthe, J. H.; van Duijneveldt, F. B. *J Chem Phys* 1984, 81, 3168.
- Bussery, B.; Wormer, P. E. S. *J Chem Phys* 1993, 99, 1230.
- Cybulski, S. M.; Burcl, R.; Chalasinski, G.; Szczesniak, M. M. *J Chem Phys* 1995, 103, 10116.
- Cybulski, S. M.; Burcl, R.; Szczesniak, M. M.; Chalasinski, G. *J Chem Phys* 1996, 104, 7997.
- Kendall, R. A.; Chalasinski, G.; Klos, J.; Bukowski, R.; Severson, M. W.; Szczesniak, M. M., Cybulski, S. M. *J Chem Phys* 1998, 108, 3235.
- Møller, C.; Plesset, M. S.; *Phys Rev* 1934, 46, 618.
- Amos, A. T.; Grispin, R. J. *Mol Phys* 1976, 31, 159.
- Jeziorski, B.; van Hammert, M. *Mol Phys* 1976, 31, 713.
- Musher, J. J.; Amos, A. T. *Phys Rev* 1967, 31, 164.
- Broussard, J. T.; Kestner, N. R. *J Chem Phys* 1970, 53, 1507.
- Broussard, J. T.; Kestner, N. R. *J Chem Phys* 1973, 58, 3593.
- Uhlrich, B. T.; Ford, L.; Browne, J. C. *J Chem Phys* 1972, 57, 2906.
- Meyer, W.; Frommhold, L. *Theor Chim Acta* 1994, 88, 201.
- Jochemsen, R.; Berlinsky, A. J.; Hardy, W. N. *Can J Phys* 1984, 62, 751.
- Hardy, W. N.; Morrow, M.; Jochemsen, R.; Statt, B. W.; Kubik, P. R.; Marsolais, R. M.; Berlinsky, A. J.; Landesman, A. *Phys Rev Lett* 1980, 45, 453.
- Knowles, D. B.; Murrell, J. N.; Braga, J. P. *Chem Phys Lett* 1984, 110, 40.
- G. Scoles, see Appendix of ref. 31.
- Das, G.; Wagner, A. F.; Wahl, A. C. *J Chem Phys* 1978, 68, 4917.
- Partridge, H.; Schwenke, D. W.; Bauschlicher, C. W. *J Chem Phys* 1993, 99, 9776.
- Dunning, T. H., Jr. *J Chem Phys* 1989, 90, 1007.
- Kendall, R. A.; Dunning, T. H., Jr.; Harrison, R. J. *J Chem Phys* 1992, 96, 6796.
- Woon, D. E.; Dunning, T. H., Jr. *J Chem Phys* 1994, 100, 2975.
- Frisch, M. J.; Trucks, G. W.; Schlegel, H. B.; Gill, P. M. W.; Johnson, B. G.; Wong, M. W.; Foresman, J. B.; Robb, M. A.; Head-Gordon, M.; Replogle, E. S.; Gomperts, R.; Andres, J. L.; Raghavachari, K.; Binkley, J. S.; Gonzalez, C.; Martin, R. L.; Fox, D. J.; Defrees, D. J.; Baker, J.; Stewart, J. J. P.; Pople, J. A. GAUSSIAN-92/DFT, Rev. G.3, Gaussian: Pittsburgh, PA, 1993.
- Boys, S. F.; Bernardi, F. *Mol. Phys* 1970, 19, 553.
- Kvasnička, V.; Laurinc, V.; Biskupič, S. *Mol Phys* 1981, 42, 1345.
- Čársky, P.; Zahradník, R.; Hubač, I.; Urban, M.; Kellö, V. *Theor Chim Acta* 1980, 55, 315.
- Hirschfelder, J. O.; Meath, W. J. *J Adv Chem Phys* 1976, 12, 3.
- Jeziorski, B.; Bulski, M.; Piela, L. *Int J Quantum Chem* 1976, 10, 281.
- Claverie, P. In: Pullman, B., ed. *Intermolecular Interactions: From Diatomics to Biopolymers*; Wiley: New York, 1978; p 69.
- Klopper, W.; Noga, J. *J Chem Phys* 1995, 103, 6127.
- Szalewicz, K.; Jeziorski, B. *Mol Phys* 1979, 38, 191.
- van Mourik, T.; van Lenthe, J. H. *J Chem Phys* 1995, 102, 7479.
- Williams, H. L.; Korona, T.; Bukowski, R.; Jeziorski, B.; Szalewicz, K. *Chem Phys Lett* 1996, 262, 431.

51. Koide, A.; Meath, W. J.; Allnatt, A. R. *J Phys Chem* 1982, 86, 1222.
52. Tang, K. T.; Toennies, J. P. *J Chem Phys* 1978, 68, 786.
53. Beventi, L.; Casavecchia, P.; Volpi, G. G. *J Chem Phys* 1986, 85, 7011.
54. Faubel, M.; Kohl, K. H.; Toennies, J. P.; Gianturco, F. A. *J Chem Phys* 1982, 78, 5629.
55. Heaven, M. C. *J Phys Chem* 1993, 97, 8567.
56. Keil, M.; Slankas, J. T.; Kuppermann, A. *J Chem Phys* 1979, 70, 541.
57. Bader, R. F. W.; Essen, H. *J Chem Phys* 1984, 80, 1943.
58. Jeziorski, B.; Moszynski, R.; Rybak, S.; Szalewicz, K. In: Kaldor, U., ed. *Many-Body Methods in Quantum Chemistry; Lectures Notes in Chemistry*, vol. 52; Springer: New York, 1989; p 65.
59. Williams, H. L.; Szalewicz, K. *J Chem Phys* 1995, 103, 4586.